

# Design of Thermoacoustic Rig for the Analysis of Thermal and Hydraulic Performance of Heat Exchangers in Oscillatory Flow

Ilori O.M., Mao X., Jaworski A.J.\*

**Abstract**—This paper describes the design and fabrication of a standing wave thermoacoustic rig for specific purpose of investigating the heat transfer and pressure drop performance of thermoacoustic heat exchangers in oscillatory flow. Detailed description of the design of various components of the rig, including the representative heat exchangers and aerodynamic shapes, intended to modify the pressure drop characteristics, is given with emphasis on different capabilities of the rig and the reasons for specific choices that are made in the process of design and fabrication. Future activities with regards to the planned studies on the rig are also discussed.

**Index Terms**—Thermoacoustics, Heat Exchangers, Heat Transfer, Pressure Drop

## I. INTRODUCTION

Thermoacoustic devices are sustainable energy technologies that create acoustic power from heat input (engine or prime over) or produce refrigeration effect from acoustic power input (refrigerator or heat pump). The basic components of a thermoacoustic (TA) device are resonator, stack (for standing wave device) or regenerator (for traveling wave device), heat exchangers and acoustic driver (or linear alternator, depending on whether the device is a heat pump or an electricity generator). TA resonator encloses the internal elements i.e. the heat exchangers and the stack or regenerator as well as the environmentally friendly inert gas e.g. Helium, Nitrogen etc., which serves as the working fluid. By placing hot and cold heat exchangers at the two ends of stack (regenerator), a temperature gradient is maintained and thermoacoustic effects can take place. The acoustic power produced by TA engine can be converted to electric power or utilized to directly drive a refrigerator or a heat pump [1-2]. Thermoacoustic technology has applications in the areas such as liquefaction and re-gasification of natural gas, electricity generation,

electrical and electronic components cooling, industrial waste heat recovery and utilization, mixture separation, automotive refrigeration, and in space applications [3-7]. The choice of TA technology for these applications is primarily due to the simplicity of its construction and the perceived high reliability in its operation. These virtues result mainly from lack of moving parts and readily available construction materials.

Despite the advantages of TA technology, there are still engineering challenges in its design and development that are yet to be completely overcome. The major challenges are in the area of heat transfer and fluid flow processes within the internal elements of a typical TA system, where the compressible fluid under oscillatory flow conditions thermally interacts with the solid boundaries such as heat exchangers and stacks (regenerators), resulting in various nonlinear flow phenomena such as vortex formation and shedding, turbulence, streaming, entrance effects etc. [2, 8-10], as well as complex heat transfer mechanisms that are yet to be fully understood. Without addressing these challenges the performance of TA systems will be degraded [11]. At present the efficiency of a typical TA engine is still about 49% of the Carnot efficiency i.e. 32% thermal efficiency [12].

Heat exchanger (HX) is an energy transfer component of TA system, through which heat is supplied (hot heat exchanger) or removed (cold heat exchanger) from the system. This simply means that the effectiveness of HX will directly translate to the improvement of overall efficiency of the TA system. However, due to the oscillatory nature of flow coupled with the effect of pressure on the gas temperature in the TA system, standard steady flow design methodologies for compact HX cannot be applied directly for the design of TA heat exchangers [13]. Hence, the heat transfer and pressure drop data that take into account nonlinear effects is still lacking. Clear understanding of the complex energy transport in and around the HX in oscillatory flow is required for the design and development of novel heat exchangers for the next generation of thermoacoustic devices.

This paper discusses the design and fabrication of a thermoacoustic rig that is specifically made for the detailed analysis of heat transfer and pressure drop performance of heat exchangers under oscillatory flow conditions. The description includes detailed design methodology,

Manuscript received March 06, 2013. This work is part of PhD research work of Ilori, O.M, sponsored by the Petroleum Technology Development Fund (a parastatal of the Ministry of Petroleum Resources in Nigeria), under the award number PTDF/E/OSS/PHD/IMO/395/11.

\* Corresponding author, Tel:- +44 (0) 116 223 1033,  
E-mail: [a.jaworski@le.ac.uk](mailto:a.jaworski@le.ac.uk)

measurement capability, test-section components consisting of two different geometries of heat exchangers and the aerodynamic shapes for optimization study. Also, future works in the standing wave rig are detailed out and conclusions are drawn based on the milestones achieved in the research so far.

## II. DESIGN METHODOLOGY

The standing wave thermoacoustic rig (Fig. 1) consists of the acoustic driver, constant cross-section resonator and the test section. From experimental point of view, standing wave rig is attractive for detailed analysis of core components such as heat exchangers, due to its simplicity.

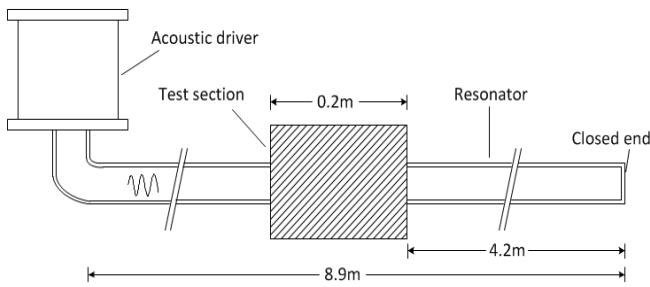


Fig. 1: Schematic of drawing of the standing wave test rig.

Practical thermoacoustic devices often operate at high pressures because power density is proportional to the mean pressure in the system [1], thus the rig is designed to use helium gas at mean pressure up-to 40bar. Based on the operating frequency of the driver (60Hz), the rig is chosen to operate at frequency of 57Hz. At this frequency, the total length of the rig is 8.9m, corresponding to a  $\frac{1}{2}\lambda$  (half-wavelength). Helium gas is selected for use in the rig. This is due to its low viscosity and high speed of sound, which is favourable for practical thermoacoustic applications. The specified operating pressure will mainly allow heat exchangers to be studied at a wide range of mean pressures. Water-heated and water-cooled HXs are designed to be investigated at temperatures in the range of 15°C to 80°C. Water-heated HX are essential in the TA systems that are built to use low grade heat sources e.g. industrial waste stream at temperatures above ambient, while the water-cooled HX are essential in TA system for wide range of applications. Detailed discussion about the HXs will be given in the section below.

### A. Acoustic Driver and Resonator

The acoustic driver here is a commercially available linear Alternator from Q-drive. Table -I gives the specifications of the driver. Since both low and high amplitude investigations on different configuration of heat exchangers will be conducted, a high-impedance transducer is chosen and located at a high acoustic impedance point in the standing wave [1]. To protect the acoustic driver from overheating and to allow easy coupling to the resonator, high pressure housing is designed for the linear alternator such that the displacement amplitude can be monitored through an optical window. The high power of the driver will facilitate the test of HXs under wide range of drive ratio

up to 10%. Drive ratio is the ratio of the pressure amplitude to that of the mean pressure in the system.

The steel resonator as used here is necessary for defining the phase of pressure and velocity of the oscillating helium gas that interacts with the boundaries of the three HXs in the

TABLE I  
SPECIFICATIONS OF ACOUSTIC DRIVER

Parameter	Unit	Magnitude
Operating current	A	3.5
Input power	Watt	275
Output power	Watt	225
Operating frequency	Hz	60
Displacement	mm	7.15
Force	N	300
Transduction coefficient	-	45.91

test section of the rig. It has a constant cross section with smooth internal surface of 52.5 mm diameter. It has joints that can be used to redefine the resonance operating frequency of the rig, if it is required at a later stage of the study, but yet the joints are few enough to keep the pressure leaks in the system to the minimum. In addition, O-rings of ferrule types are used at all joints to prevent pressure losses.

### B. Test-section designs

The test section, schematically illustrated in Fig. 2, has effective length of 200mm. It is located at the position  $x = 4.2\text{m}$  measuring from the closed end of the resonator. This position nearly corresponds with the velocity antinode. This further enables the test of heat exchanger at different velocity amplitudes. The choice of this position is to ensure a high and large range of gas displacement amplitudes. The specific features of the test section include:

- Heat leak prevention
- Built-in flexibility
- Increased measurement capability

#### Heat leak prevention

To minimise heat leak in the test section, symmetrical arrangement of HXs, internal insulation, and increased number of temperature measurement points are considered in the design. The symmetrical arrangement of HX is such that, water-heated hot heat exchanger (HHX) is centrally placed between two identical water-cooled cold heat exchangers (CHX). The two CHX's are purposely arranged this way to enable accurate estimation of heat removal from the oscillating gas, thus enabling energy balance analysis. Furthermore, identical set (CHX-HHX-CHX) are chosen for the symmetry in order to minimise nonlinear effect associated with geometrical discontinuity [8].

The heat balance that will result from this arrangement can be expressed as

$$\dot{Q}_h = 2\dot{Q}_c + \dot{Q}_l \quad (1)$$

where,  $\dot{Q}_h$  is the heat input through the HHX,  $2\dot{Q}_c$  is the heat removed by the two CHX's and  $\dot{Q}_l$  is the heat losses. In addition to heat leak prevention, symmetrical arrangement of HXs will also protect acoustic driver from overheating (max. temperature = 45°C).

An internal insulation method is adopted for the test section design. The volume enclosed by the internal surface of the housing and the external surfaces of HXs and the spacers will be filled with insulation material such Insulfrax S blanket. This will further ensure that heat leak is prevented and it provides an opportunity for external insulation if it is later required.

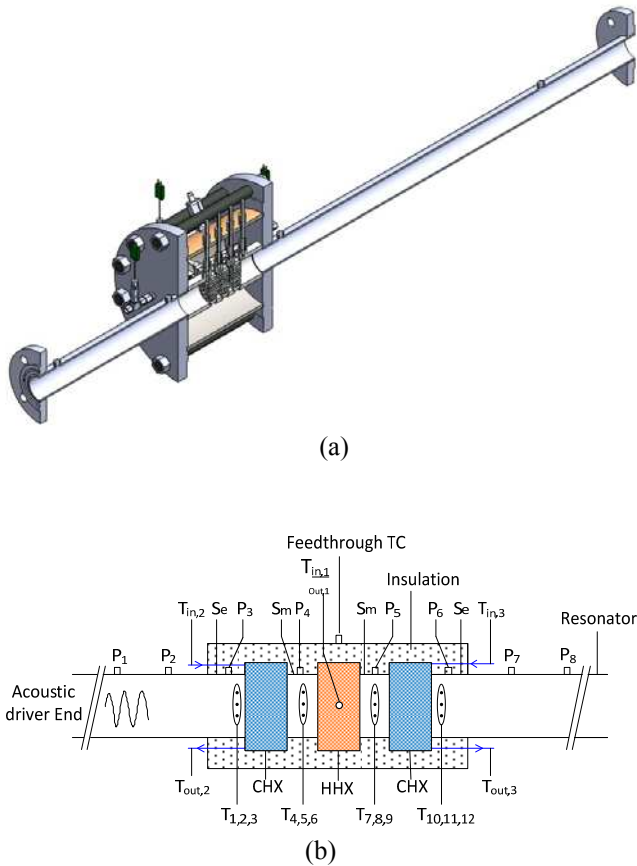


Fig. 2: Test section of standing wave test rig. (a) CAD-Image Illustration. (b) Schematic drawing illustration. HHX and CHX are water-heated and water-cooled heat exchangers respectively. P1 to P8 are pressure sensors located in the resonator and test section. T1 to T12 are the type-K temperature sensors in the test section.  $T_{in,1}$ ,  $T_{out,1}$ ,  $T_{in,2}$ ,  $T_{out,2}$ ,  $T_{in,3}$  and  $T_{out,3}$  indicate the thermocouple locations at inlet and outlet of the hot and two cold heat exchangers respectively.  $S_m$  and  $S_e$  are middle and end spacers respectively.

#### Built-in flexibility

The test section is sized such that the HXs sizes and the gap between them can be changed easily without the need to resize the whole test section. Also, instrumentation for parameter measurements (e.g. gas velocity amplitude) and the turbulence generators can be easily introduced. This feature is important for future research requirements, as it allows in-depth parametric study on the HXs.

The main test-section components are the housing and spacers. They can be further described as follows:

#### A. Housing

Housing encloses one HHX, two CHX, and the spacers, clamped in between two 8-inch flanges that connect the test-section to the rest of the resonator, using studs and nuts. It is fabricated from 8-inch weldpipe sch-40 316SS and has a total length of 206mm. The in-built flexibility feature of the rig is derived partly from the housing design. It was sized such that it conveniently accommodates HXs of different

sizes, the spacers and the fittings for water inflow and outflow, and designed to allow access for pressure and temperature measurement. Grooves of 3.5 x 1.5 mm (WxD) are made on the flat circular edges for 8-inch O-ring of 3mm cross section for the pressure seal.

#### B. Spacers

Four spacers are designed to be used in the test section, two middle-spacers and two end-spacers. The middle spacers separate the HHX from the two CHXs and the end-spacers separate the CHXs from the inner wall of the 8-inch flanges. The spacers, both the middle and end provide a continuation of the resonator through which the helium gas oscillates. Each spacer has inner diameter of 57.4 mm and thickness of approximately 8.8 mm. An interesting feature of the spacers is the pressure sensor holder, through which the dynamic pressure sensors will be installed. The design is such that the pressure sensors will be flush mounted (Fig. 3) at distance 7.5 mm from the nearest HX. The choice of this location is to enable time-dependent measurement as close as possible to the HX inlet and outlet. Using differently sized spacers, the gap between HXs can be varied to suit different measurement requirements. To minimize heat conduction from gas side to insulation material side, Nylon-6 (0.23W/m.K) is selected for the material out of which the spacers are fabricated.

### III. MEASUREMENT CAPABILITY

#### A. Pressure measurement

In order to directly measure the acoustic pressure drop across each of the HXs (Fig. 2), the test-section is designed such that the pressure sensors will be installed within the high pressure environment without exposing the sensors to the pressurized helium gas in the test section (Fig. 3). Using this installation method, the sensor cables can be run from the process side through 8 mm stainless tube and standard fittings to connect the data acquisition card outside the test section. In all, four sensors (P3, P4, P5 and P6) are located in the test section and the distance between two adjacent pressure sensor ports is 32 mm. The reference pressure ( $P_0$ ) is to be measured at the closed end of the resonator (Fig. 1). This point corresponds to the pressure antinode for a half-wavelength rig.

#### B. Velocity measurement

In addition to the four pressure sensor ports that are located within the test section for acoustic pressure measurement, separate four pressure ports (Fig. 2) are in the resonator for velocity amplitude measurement (two ports on either side of the test section). The method of velocity amplitude measurement described by Fusco et.al [14], commonly referred to as Two-microphone method [2], is of interest here for the initial measurements. Pressure ports P1 and P2 are separated by 300 mm gap, while P7 and P8 are 700 mm away from each other. The locations of these pressure ports are influenced by the consideration for velocity amplitude measurement on either side of the test-section.

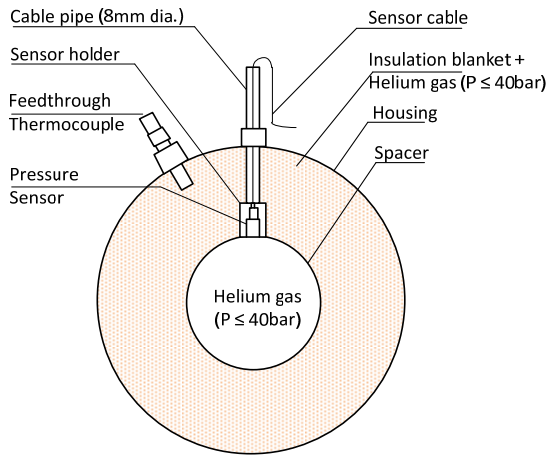


Fig. 3: Section view of pressure sensors and feedthrough thermocouple arrangements in the test section

### C. Temperature measurement

High Density Feedthrough assembly with 20-pairs of 0.5mm diameter type-K thermocouple and PTFE sealant is used in the test-section for temperature measurement in the acoustic environment. Having large number of temperature probes is thought to be beneficial in this study as detailed heat transfer performance is of primary interest, accurate account of heat gain/loss in and around the HX need to be provided. Inlet and outlet temperatures on the water side of both HHX and CHX are designed to be measured with six 0.5 mm diameter type-K thermocouples by immersing them in the water flow path using standard fittings. In addition, the use of feedthrough assembly for thermocouples offers the advantage of minimizing the pressure and heat leaks which may result from drilling large number of holes in the housing, and heat conduction through a large number of fittings.

## IV. TEST OBJECTS

The test objects here are mainly the heat exchangers and the shape optimization kits. Combining the HX and aerodynamic shapes as depicted in Fig. 4 is to allow reliable measurements and combination of heat transfer, pressure drop and optimization studies of the HX in the purpose designed and built standing wave rig.

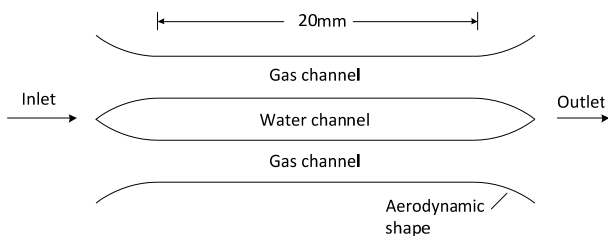


Fig. 4. Heat exchanger channels and the created end effects by aerodynamic shape.

### A. Heat Exchangers

Commonly studied thermoacoustic HXs include parallel plate, compact (conventional) shell and tube and others. Various configurations of HXs were examined within the framework of the preliminary design consideration in this study. Tube-Heat exchanger (THX) and Finned-Heat exchangers (FHX) were selected, designed and fabricated

TABLE II  
HEAT EXCHANGERS GEOMETRICAL PARAMETERS

Channels	Unit	Tube-Heat Exchanger (THX)	Finned-Heat Exchanger (FHX)
<i>Gas channel</i>			
Tube length	mm	20	-
Number of circular holes	-	89	-
Hole diameter	mm	3	-
Slot length	mm	-	20
Slot height	mm	-	3
Number of slots	-	-	9
Porosity	%	32.04	75.7
Separation wall thickness	mm	0.5	0.5
Frontal diameter	mm	50	50
<i>Water channels</i>			
Width	mm	12	12
Height	mm	1.5	1.5
Length	mm	67	67
Number of channel	-	10	10

for the initial heat transfer and pressure drop analyses in the acoustic environment. Table -II shows the specifications of the two types of HXs that are chosen for the initial study. Both are water-heated and water-cooled, cross flow types. Their gas channel patterns are same as shown in Fig. 5a and 5b. Plain flat-crest fins of regular rectangular cross section are used in the FHX (not shown in Fig. 5b). The water channels are similar in both HXs (detail of the water channels not shown in Fig. 5). The arrangements of the HXs as will be tested are shown in Fig. 2 and discussed in the section for 'Heat leak prevention'. The HXs are located at distances 58, 90, and 122 mm measuring from the inner wall of 8-inch flange on acoustic driver side (Fig. 1). The distance between two adjacent HXs is 12 mm for this initial arrangement.

Each type has its porosity calculated based on continuous flow passage from the following expressions

$$\phi_{THX} = \frac{A_o}{A_f} = \frac{nd_g^2}{D_f^2} \quad (2)$$

$$\phi_{FHX, no-fin} = \frac{\pi r_g l_i}{A_f} \quad i = 1, 2, \dots, 9 \quad (3)$$

Where  $A_o$ ,  $A_f$ ,  $D_f$ ,  $n$ ,  $d_g$ ,  $r_g$ , and  $l_i$  are the minimum free-flow cross-sectional area, frontal core area and frontal core diameter for THX and FHX, number and diameter of gas channels for the THX, gas channel edge-radius and length (perpendicular to flow direction for the FHX).

Thermal penetration depth is an important parameter in the design of HXs, it is defined as:

$$\delta_k = \sqrt{\frac{2k}{\omega \rho c_p}} \quad (4)$$

where  $k$ ,  $\rho$ , and  $c_p$  are the thermal conductivity, density and specific heat capacity of the helium gas,  $\omega = 2\pi f$  ( $f$  is the operating frequency), is the angular frequency. The tube radius of THX and gas channel height of FHX are chosen to be  $\sim 9.375\delta_k$ . At the frequency of 57 Hz, and mean pressure

ranging from atmospheric to 40 bar, the calculated thermal penetration depths range from 1.002 mm (at atmospheric pressure) to 0.16 mm (at mean pressure of 40 bar). Therefore, the radius of THX gas channel is 1.5mm and the channel height of FHX is 3 mm, at mean pressure of 40 bar. The choice of this value is to allow a larger range of flow and heat transfer study on the HXs, since the thermal penetration depth is inversely proportional to the mean pressure in the system [15]. The lengths of the HXs are normally estimated from the peak-to-peak displacement amplitude  $2\xi$  [1], however, we chose to use length of 20 mm in the fabrication, which is in-line with the previous studies and will allow a comparison with previously tested HX [16-17]. The overall size of the HX, that is, the frontal core is influenced mainly by the inner diameter of the resonator and the consideration for ensuring constant cross-section of the resonator. Aluminium material is used for fabrication of both heat exchangers mainly because of thermal conductivity and machinability considerations.

### B. Aerodynamic shapes

As part of the optimization of heat exchangers in this study, aerodynamic shapes (Fig. 5) have been designed and fabricated as separate plates to provide aerodynamic effects at the gas channel entrance and exit of THX and FHX. The patterns are the same with that of HXs they will be attached to. The reason for using plate attachments for producing the aerodynamic shapes is simply the flexibility that such method offers. Using separate plates will enable different shapes with large range of aspect ratios to be designed, fabricated and studied without having to fabricate large number of heat exchangers.

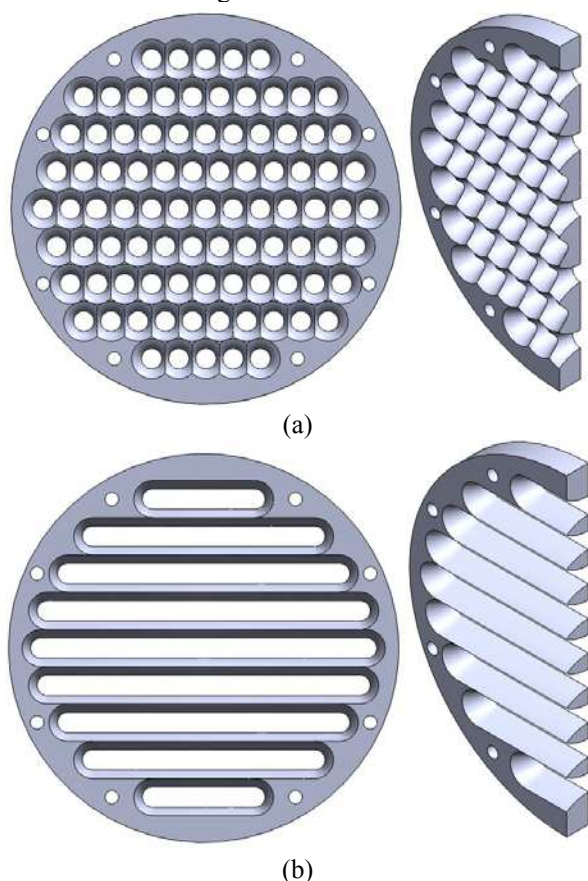


Fig. 5: CAD-Image of aerodynamic shapes. (a) THX pattern and the created edge effect. (b) FHX pattern and the created edge effect.

The designed aerodynamic shapes have curvature ranging from 0.5mm to 7.0mm. The curvatures are chosen as arcs of circles with known radii. The plate thickness (corresponding to the chord length) of 1mm is used for 0.5 mm curvature while 4mm plate thickness is used for 7mm curvature. The maximum heights (distance normal to the cord length) are 1.25mm and 1.45mm for THX and FHX respectively. The aerodynamic shape here is such that symmetry between the entrance “Leading edge” and exit “Trailing edge” of the HX is maintained, so that the same platform can be established for monitoring the flow conditions at the entrance and exit of the HXs.

### Fabrication

For the HXs, the gas channels are fabricated using CNC machine. The water channels of both HXs are fabricated using spark-erosion machining technique. This is a machining technique whereby a desired shape is obtained using electrical discharges (sparks), to remove material from the work-piece by a series of rapidly recurring current discharges between two electrodes, separated by a dielectric liquid and subject to an electric voltage. The choice of this technique for the HXs is because of the length of the rectangular channel (67mm) coupled with the thin separation wall (0.5 mm) requirement and the channel height (1.5 mm).

A typical aerodynamic shape is produced by pre-fabricating the required profile with desired aspect ratio as a tool. The tool is fabricated such that it takes into account the accuracy of the final profile dimensions in the aerodynamic shape. The patterned tool is attached to the machine and the profile on it is machined on a plate of appropriate thickness using spark erosion technique to achieve the production. The production begins with operating current of 21 Amps which give a coarse surface finish. The profile is further smoothed to achieve precise profile dimensions and quality surface finish by decreasing the operating current to 4 Amps which gives acceptable level of surface finish. Decreasing the operating current further is possible but with huge ‘cost’ of production time. This method of manufacturing is adopted, as the conventional milling method could not be used to achieve the required profile of the aerodynamic shapes.

### V. CONCLUSIONS AND FUTURE WORK

This work discusses the design and fabrication of standing wave thermoacoustic test rig for a study of fundamental problem of heat transfer and pressure drop performance of thermoacoustic heat exchangers under oscillatory flow conditions. Test rig, including representative heat exchangers and the optimization kits has been designed and fabricated, and is to be tested in a range of acoustic amplitude conditions.

Future research works will focus on experimental measurements in the described standing wave rig. Experimentally, the effect of operating parameters (i.e. gas mean pressure, mean temperature, displacement amplitude, and drive ratio) and geometrical parameters (i.e. length of heat exchanger, gas channel radius and height, and spacing between two adjacent heat exchangers) on heat transfer and pressure drop performance of heat exchangers in oscillatory flow will be investigated. In addition, optimization study

will be conducted with the use of turbulence generators and aerodynamic shapes attached to the entrance and exit of the heat exchanger channels. For the aerodynamic shape, the effect of radius of curvature on heat exchanger performance will be considered. Heat transfer and pressure drop will be evaluated in terms of non-dimensional parameters such as Nusselt numbers, drag coefficients etc.

#### REFERENCES

- [1] Swift, G.W., Thermoacoustics: A unifying perspective for some engines and refrigerators. Los Alamos National Laboratory, 2001(Fifth draft, LA-UR 99-895).
- [2] Swift, G.W., Thermoacoustic engines *Journal of Acoustical Society of America*, 1988. 84(4).
- [3] Adeff Jay A., H.T.J., Design and construction of a solar powered, thermoacoustically driven, thermoacoustic refrigerator. *J. Acoust. Soc. Am.*, 2000. 107(6).
- [4] Wollan, J.J., et al., Development of a Thermoacoustic Natural Gas Liquefier. Presentation at 2002 AIChE New Orleans Meeting, New Orleans, , 2002. LA-UR-02-1623.
- [5] Symko, O.G., et al., Design and development of high-frequency thermoacoustic engines for thermal management in microelectronics. *Microelectronics Journal*, 2004. 35(2): p. 185-191.
- [6] Spoor, P.S. and G.W. Swift, Thermoacoustic Separation of a He-Ar Mixture. *Physical Review Letters*, 2000. 85(8): p. 1646-1649.
- [7] Luke, Z., et al., Feasibility Study of an Automotive Thermoacoustic Refrigerator. *Proceedings of Acoustics*, Busselton, Western Australia, 2005.
- [8] Jaworski, A.J., et al., Entrance effects in the channels of the parallel plate stack in oscillatory flow conditions. *Experimental Thermal and Fluid Science*, 2009. 33(3): p. 495-502.
- [9] Mao, X., et al., PIV studies of coherent structures generated at the end of a stack of parallel plates in a standing wave acoustic field. *Experiments in Fluids*, 2008. 45(5): p. 833-846.
- [10] Mao, X. and A.J. Jaworski, Application of particle image velocimetry measurement techniques to study turbulence characteristics of oscillatory flows around parallel-plate structures in thermoacoustic devices. *Measurement Science and Technology*, 2010. 21(3): p. 035403.
- [11] Gardner, D.L. and G.W. Swift, A cascade thermoacoustic engine. *The Journal of the Acoustical Society of America*, 2003. 114(4): p. 1905.
- [12] Tijani, M.E.H. and S. Spoelstra, A high performance thermoacoustic engine. *Journal of Applied Physics*, 2011. 110(9): p. 093519.
- [13] Garrett. S.L., Perkins D.K., and G. A., Thermoacoustic Refrigerator Heat Exchanger- Design, Analysis and Fabrication. *Proc. of the Tenth International Heat transfer Conference*, Brighton, UK, 1994.
- [14] Fusco Andrew M., Ward William C., and S.G. W., Two-sensor power measurements in lossy ducts. *Acoustical Society of America*, 1992. 91(4).
- [15] Belcher, J.R., et al., Working gases in thermoacoustic engines. *Journal of Acoustical Society of America*, 1999. 105(5): p. 2677-2684.
- [16] X. Mao, W. Kamsanam, and A.J. Jaworski, Convective Heat Transfer from Fins-On-Tubes Heat Exchangers in An Oscillatory Flow. *Proc. 23rd IIR International Congress of Refrigeration*, 2011. ID: 589.
- [17] Kamsanam W, M. X., and J.A. J., Heat Transfer Performance of Finned-Tube Thermoacoustic Heat Exchangers in Oscillatory Flow. *ICSV19 Vilnius, Lithuania*, 2012.
- [18] Marx David, Bailliet Helene, and V. Jean-Christophe, Analysis of acoustic flow at abrupt change in section of waveguide using Particle image Velocimetry and Proper Orthogonal Decomposition. *Acta Acustica United With Acustica*, 2008. 94: p. 54-65.
- [19] Tijani M.E.H., Z.J.C.H., de Waele A.T.A.M., Design of thermoacoustic refrigerators. *Cryogenics* 2002. 42 p. 49–57.